

New Modality for Maximizing Cryosurgical Killing Scope While Minimizing Mechanical Incision Trauma Using Combined Freezing-Heating System

Jing-Fu Yan

Zhong-Shan Deng

Cryogenics Laboratory,
Technical Institute of Physics and Chemistry,
Chinese Academy of Sciences,
P.O. Box 2711,
Beijing 100080, P.R.C.

Jing Liu¹

Cryogenics Laboratory,
Technical Institute of Physics and Chemistry,
Chinese Academy of Sciences,
P.O. Box 2711,
Beijing 100080, P.R.C.;
School of Medicine,
Department of Biomedical Engineering,
Tsinghua University,
Beijing 100084, P.R.C.
e-mail: jliu@cl.cryo.ac.cn

Yi-Xin Zhou

Cryogenics Laboratory,
Technical Institute of Physics and Chemistry,
Chinese Academy of Sciences,
P.O. Box 2711,
Beijing 100080, P.R.C.

Cryosurgery is a minimally invasive surgical technique using extremely low temperature to destroy undesired tissues. A surgical freezing margin of at least 1 cm is often recommended to avoid local tumor recurrence after surgery. For treating slender or elongated solid tumors in a conventional cryosurgery, simultaneous insertion of multiple cryoprobe is a necessity to guarantee an adequate killing scope. However, the risk of mechanical incision trauma may outweigh the benefits of such therapy. To resolve this difficulty, we proposed a new cryosurgical treatment modality, which can significantly maximize the killing scope while minimize the incision trauma, using the recently developed combined cryosurgical-hyperthermia treatment system (CCHTS). The method, named as one time's percutaneous insertion while multiple times' freezing/heating ablation, is rather flexible in administrating a complex cryosurgical process and avoids certain shortcomings of conventional freezing strategies. Owing to the powerful heating function, the present probe can be easily moved back along its original incision tract to the desired positions immediately after initiating the heating. Then, a new iceball can be formed there while the iceballs generated before still remain unmelted in the following cycles. Consequently, a slender iceball could be generated to embrace the whole elongated tumor. This is, however, rather hard to achieve for a conventional cryosurgery with only one single freezing function or using only one probe. To visually demonstrate the feasibility and potential advantage of the present method, proof of concept in vitro gel experiments were performed. In addition, tests and corresponding theoretical simulations were performed on pork tissues. All the results indicate that the elongated iceball could be easily generated by using only one CCHTS probe owing to its strong freezing/heating capability. In this way, a large number of incisions with multiple probes, commonly adopted in a conventional cryosurgery, can be avoided and the serious mechanical trauma including potential dangers can thus be significantly reduced. Meanwhile, the cost for the operation and postmedical care will be lowered. The present strategies are expected to be valuable in administrating a highly efficient and minimally invasive cryosurgery in the near future. [DOI: 10.1115/1.2812423]

Keywords: cryosurgery, hyperthermia, combined treatment, minimally invasive system, tumor destruction, treatment planning, mechanical trauma

1 Introduction

Cryosurgery, also known as cryoablation or cryotherapy, is a minimally invasive surgical technique, which uses very low temperature to destroy diseased tissues. As an alternative to radiotherapy in the mid-1960s [1–4], it was, however, abandoned more or less due to a high incidence of complications resulted from difficulties in guiding and controlling the freezing process. Until the early 1990s, technological advances stimulated the renewed interest of the cryosurgery [2,5–8]. A safer and more effective cryosurgical procedure has now been available, such that surgeons can better target the diseased region and control the freezing just on the right site. Usually, a spinal anesthesia is required and the entire procedure takes about 2 h. Cryosurgery has potential advantages over other methods in tumor treatment [9–13], such as small incision, short period of time on an outpatient basis, low

blood loss and pain, no added morbidity, and so on. The major disadvantages of cryosurgery are its uncertainties of long-term effectiveness and efficacy of the procedure [12–14].

Generally, the outcome of a cryosurgery is strongly dependent on the cooling rates imposed, as well as the lowest temperatures reached [3,4,12,15–19]. Meanwhile, duration and number of repetitions are also important factors responsible for the entity of the damage. In addition, for treating a slender solid tumor, it is important to effectively cover the whole solid tumor by generating an elongated iceball with a desired shape in order to minimize the reoccurrence rate. However, with most of the previously developed cryoprobe systems, which are only capable of performing a single freezing function, it is rather difficult and inconvenient to solve this problem. Multiple-probe approach is therefore a most important choice to adapt to an elongated tumor. However, with the dramatically increasing numbers of multiple probes, regardless of using either liquid nitrogen cooling (Erbe Elektromedizin GmbH, Germany) or Joule-Thomson cooling (Endocare, Inc., CA; Galil-Medical, Inc., Israel), a new level of difficulty appears. That is, operation of multiple cryoprobes could bring additional

¹Corresponding author.

Manuscript received January 25, 2007; final manuscript received September 19, 2007. Review conducted by Vijay Goel.

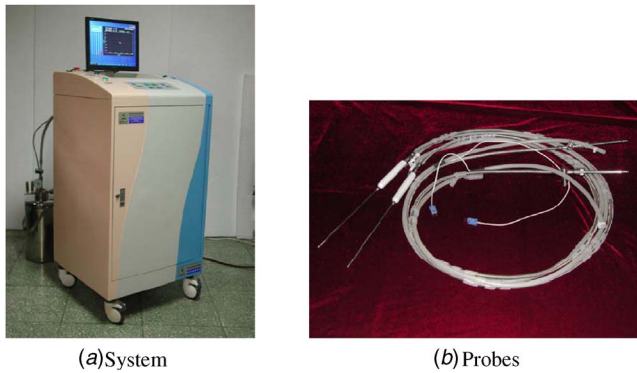


Fig. 1 The new CCHTS

serious mechanical incision traumas to the surrounding healthy tissues. In order to resolve such difficulty, we proposed a new modality based on our newly developed equipment, named as combined cryosurgical-hyperthermia treatment system (CCHTS) (Fig. 1) [23]. Considering the fact that freezing immediately followed by a rapid and strong heating would significantly improve the destructive effect [20–22], CCHTS is aimed to increase the efficacy of conventional cryosurgery. Compared with other currently available cryosurgical instruments, this new system could provide stable and strong heating performance. Readers are referred to Ref. [23] for more detail.

The feasibility of the new modality as proposed in the present paper is guaranteed by fully taking use of the strong heating performance of the CCHTS. This approach, which can be termed as one time's percutaneous incision and multiple times' freezing/heating ablations, will be described as follows. The probe can be easily pulled back via a safe way immediately after the heating was initiated. When an iceball is formed, a strong heating would quickly thaw the tissues there, which in return allows the probe to be easily moved to the other places. After that, one can administer a new freeze-heat cycle at the new position as desired. With this moving freezing and heating pattern, a slender tumor, originally unable to be covered by the initial cycles, can now be completely frozen and heated in the subsequent cycles. It is by way of the alternative freezing/heating and movement of the probe (Fig. 2) that a large iceball with desired gourd shape was formed. Most importantly, this was achieved using only one probe via a single percutaneous incision. Previously, some researchers had tested a similar idea using the pull-back method [24,25], which later turns out as a gold standard in prostate cryosurgery. The major difference between the present method and the former pull-back strategy lies in that the treating procedure here is possible by only using the powerful heating function (reaching 85°C within 60 s after freezing was stopped) as provided by the CCHTS. This makes a large scale freezing and heating ablation rather quick and reliable.

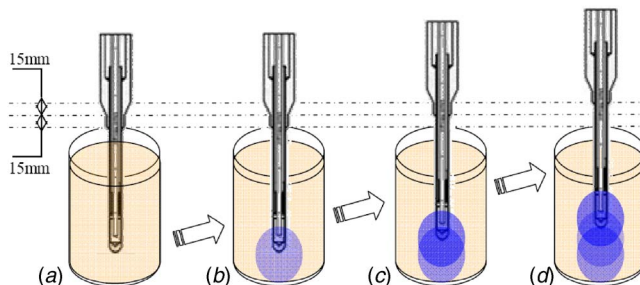


Fig. 2 Subsequent iceball formation in gel using freezing/heating probe

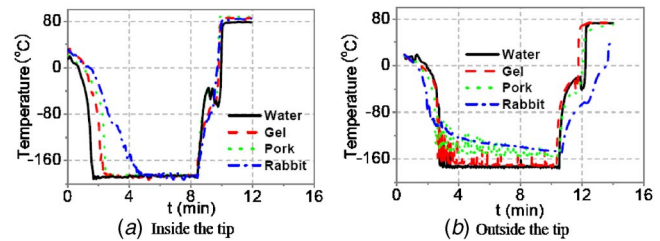


Fig. 3 Temperature responses of cryoprobe when freezing/heating various materials

Compared to the multiple-probe approach in a conventional cryosurgery, the present modality appears more flexible in treating a slender tumor. In addition, the strong heating feature of the CCHTS cannot only evidently shorten the rewarming time for the pullback but also guarantee the safety of moving probe so as to prevent metastasis. In order to demonstrate the feasibility as well as potential advantages of this new modality, a series of proof-of-concept experiments and corresponding numerical simulations were performed in this study.

2 Methods and Results

2.1 Performance Test of Combined Cryosurgical-Hyperthermia Treatment System.

Although a large amount of experimental data are available, only some typical results reflecting the quick heating features of CCHTS on frozen tissues will be given here. Figure 3(a) represents the temperature transients inside the tip of one 5 mm cryoprobe, which was inserted into different kinds of experimental samples during the freezing and heating process in one cycle. As a comparison, the temperature outside the tip of one 5 mm cryoprobe corresponding to Fig. 3(a) was also shown in Fig. 3(b), reflecting the real temperature response of tissues immediately contacting the probe tip. From Fig. 3(b), one can find that different samples take various responses under the same freezing and heating condition. Clearly, in water, gel, and pork, the working performance of the system is fairly good. The freezing rate stays at about 90°C/min, while the heating temperature can reach 85°C within only 60 s, which, however, can hardly be realized by a conventional cryosystem. For the in vivo experiments, the tissue temperature only decreases a little bit slower than the former case during freezing process. However, it still falls to -180°C within 5 min. The heating rate still keeps high in the tissue (reaching 80°C within 2 min after freezing was stopped), though a little bit slower than that of in vitro experiment. Regardless of the fact that there appears a small fluctuation when maintaining the maximum or minimum temperatures, it still could hold the temperature in a relative stable level, which fully proves the powerful heating performances of the whole system. In cryosurgery, a widely accepted killing temperature is about -40°C, while in hyperthermia, the effective killing temperature is above 42°C. Based on these two temperatures, we test the new system's freezing/heating capacity through in vivo experiment on anesthetized rabbit, with a weight of about 3 kg. Two cryoprobes with 5 mm diameter are percutaneously inserted into the target area (rabbit thigh) within a depth of about 15 mm. Figures 4(a) and 4(b), respectively, depict the thermocouple distributions and snapshot in rabbit thigh experiment. Here, the temperature responses at the pinheaded Thermocouples 3, 4, 5, 6, 7, and 10, which are surrounding probe 2 and inserted to the perpendicular depth of about 10 mm, are recorded, respectively. From Fig. 4(a), it can be found that Thermocouples 3 and 7, and 4 and 6 are symmetrically positioned in the nearby of the surrounding cryoprobes. Therefore, the temperature transients of Thermocouples 3 and 7 and Thermocouples 4 and 6 are expected to develop via a similar way. The experimental results are given in Fig. 5, which basically accords with what has been anticipated. Depending on the killing criteria

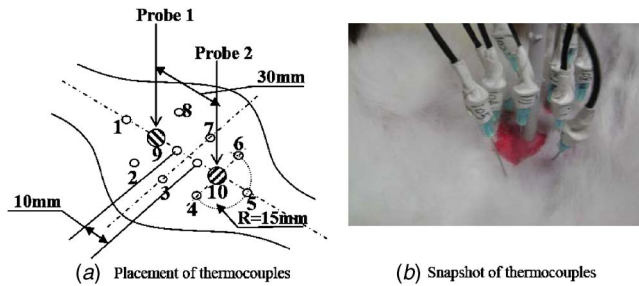


Fig. 4 In vivo experiment on rabbit thigh

as mentioned above, the tissues even at the far position of Thermocouple 7 can be possibly damaged only after about 5 min freezing. The heating effect is not obvious because the heating time is still not long enough (only 150 s). However, from curves of Thermocouple 10, the temperature has reached 42°C within a very short period of heating. All these animal results indicate the excellent heating performance of the new system, which guarantees the flexible movement of the probe along its incision tract in the frozen tissues.

In a conventional cryosurgery, the tumor is often frozen for a desired duration time and the freezing is then stopped for several minutes. This procedure would be repeated several times or only once depending on the experience of cryosurgeon and performances of the freezing device. Due to lack of rewarming feature in previous cryosurgical instruments, once multiple cryoprobes were inserted into the right place and the target tissues were deeply frozen, moving the probes for a desired conformable treatment could be extremely difficult. That is especially true for treating tumors with elongated shape. In order to better adapt to slender tumors, most of the cryosurgeons just choose to perform cryosurgery with multiple probes, which could cause strong mechanical injuries. Moreover, it would increase the complexity of the cryosurgical operation as well as the medical cost. Compared with this, the new system suggests an efficient way to resolve the above difficulty.

2.2 Demonstration Experiments on New Modality. In order to demonstrate the new modality of the combined freezing/heating system for maximizing cryosurgical killing scope while minimizing invasive trauma, a series of conceptual experiments were performed as follows.

In the first experiment, one probe with diameter of 5 mm was operated by three times' freezing coupled with subsequent heating when pulled back along its incision tract. What presented in Fig. 6

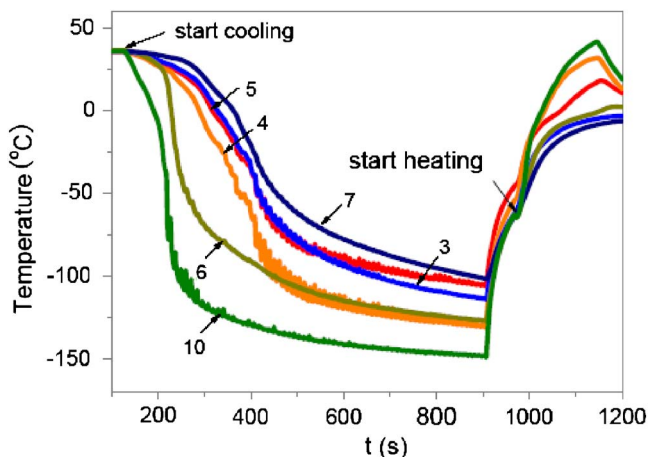


Fig. 5 Temperature responses of rabbit thigh tissue at selected positions during one freezing/heating cycle

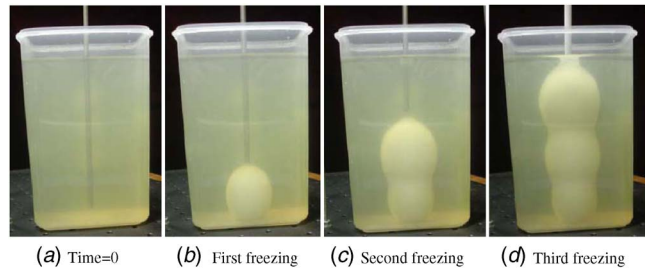


Fig. 6 Visual pictures for subsequent formation of iceball during moving freezing on phantom gel by the new system

is a straightforward validation experiment on gel, which is semi-transparent and particularly chosen here for the visual observation on the iceball formation and thawing process. The size of the iceball often determines the treatment efficiency of the cryosurgery. To monitor the dynamic information of iceball in real time, a digital camera Nikon Coolpix 880 was used to take photos at every 1 min interval. In this way, one can clearly monitor the detailed profile of the growing iceball in the transparent gel during the experiment. The whole experiment was implemented in such an order: (1) perpendicularly inserting one cryoprobe into gel with a depth of 40 mm from the surface, (2) then freezing the gel for 10 min followed by 1 min heating, and (3) pulling the cryoprobe back for 15 mm along its original incision tract and then repeating the freezing and heating as that performed in Step (2). Figures 6(a)–6(d) display the pictures at four different times (before freezing, and after the first, second, and the third freezing cycle, respectively). The results indicate that using the present modality, a nonellipsoidal iceball has been successfully generated. Clearly, through a specific combination between multiple freezing and heating cycles as well as certain particular movement of the probe, more complex elongated iceball configuration can still be realized as desired. Such property would be very beneficial to envelop slender tumors, which is critically important in clinics. Moreover, with the newly developed freezing/heating system, only one time's percutaneous incision is needed for the single probe to produce a much large and long iceball, which would better help planning a highly efficient and minimally invasive targeted treatment.

As a comparison, additional experiments were also performed on an in vitro porcine liver to further illustrate the efficacy of the new modality. The action of pulling back cryoprobe was taken at the end of each heating process and each cycle takes about 10 min freezing and 2 min heating except that the second cycle takes about 5 min freezing and 1 min heating. The snapshots at each cycle were presented in Figs. 7(a)–7(f), respectively. The probe has a diameter of 5 mm, which was transversely inserted into the tissue. Snapshots were taken from the top in order to monitor the formation of the iceball. First, the probe was moved back along the tract for a distance of about 25 mm. Second, the probe was moved backward for 20 mm. Then, probe was moved backward for 30 mm. Finally, probe was moved backward for 25 mm. Figure 7(a) indicates the iceball formation on the surface of liver at the first cycle. Due to the powerful dual freezing/heating feature of the new system, a crack was produced which indicate the damage resulted from strong thermal stress. Figure 7(b) shows iceball formation at the second cycle, from which one can see that the iceball moved backward and its contrail is along the original incision tract. Figure 7(c) presents the iceball formed at the third cycle. As a matter of fact, if one controlled the moving distance and the freezing duration time manually and properly, an overlapped iceball with the expected shape could be formed. Another merit of this new modality especially lies in that only using one probe, an iceball could easily reach 12 cm in length and 5 cm in width, as shown in Figs. 7(e) and 7(f), which is quite helpful for treating large tumors. Most importantly, probe movement control

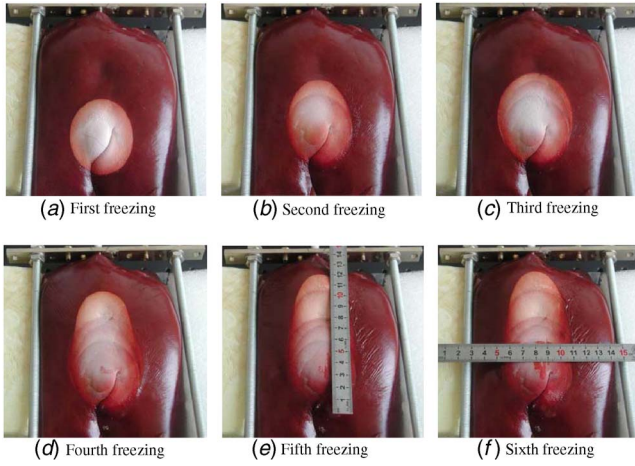


Fig. 7 Subsequent formation of iceball during moving freezing on pig liver by the combined system

of each cycle was achieved via a rather easy and fast way. There was no forcible removal and bleeding during the whole procedure. Both the above two conceptual experiments demonstrate the great potential feasibility and efficacy of the new modality combined with CCHTS to treat some special tumors at a lower cost.

2.3 Theoretical Modeling. To further interpret the new modality, the transient bioheat transfer problem involving moving freezing/heating of biological tissues with CCHTS is investigated in this section. A mathematical model is established to simulate the new modality with one probe for both in vitro and in vivo cases. Just as expected, a series of computational results show a good imitated icy gourd shaped iceball corresponding to the measurements of aforementioned experiments.

The relationship describing heat transfer in unfrozen tissue, often called the bioheat equation, involves the effects of blood perfusion and metabolic heat generation, which was first established by Pennes in the following form:

$$C_u \frac{\partial T_u(X,t)}{\partial t} = \nabla \cdot k_u \nabla [T_u(X,t)] - \omega_b C_b T_u(X,t) + Q_m + \omega_b C_b T_a \quad X \in \Omega_u(t) \quad (1)$$

where C_u and C_b are, respectively, the heat capacity of unfrozen tissue and blood; X contains the Cartesian coordinates x , y , and z ; $\Omega_u(t)$ denotes the unfrozen domain at time t ; k_u the thermal conductivity of unfrozen tissue; ω_b the blood perfusion; T_a the arterial temperature; $T_u(X,t)$ the temperature of unfrozen tissue; and Q_m the metabolic heat generation.

In the frozen region, due to the absence of blood perfusion and metabolic activities, the heat balance is expressed by

$$C_f \frac{\partial T_f(X,t)}{\partial t} = \nabla \cdot k_f \nabla [T_f(X,t)] \quad X \in \Omega_f(t) \quad (2)$$

where C_f and k_f are, respectively, the heat capacity and thermal conductivity of frozen tissue; $\Omega_f(t)$ denotes the frozen domain at time t ; and $T_f(X,t)$ the temperature of frozen tissue.

In order to avoid the time-consuming iteration at the moving boundary, the effective heat capacity method [26–33] is applied here. Based on the energy conservation model for a multicomponent phase change system, a unified equation, which can be applied to frozen, partially frozen, and unfrozen tissue regions, respectively, can be developed by introducing effective heat capacity. The final uniform energy equation for biological tissue during freezing/heating can be written as

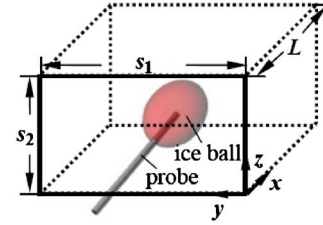


Fig. 8 Schematic of 3D geometry for one probe case

$$\tilde{C} \frac{\partial T}{\partial t} = \nabla \cdot \tilde{k} \nabla T - \tilde{\omega}_b C_b T + \tilde{Q}_m + \tilde{\omega}_b C_b T_a \quad X \in \Omega \quad (3)$$

For brevity, the derivation process of the above equation and the corresponding numerical algorithm are not repeated here. Readers are referred to Ref. [34] for more details. A schematic of the 3D calculation geometry for the one probe case in vitro or in vivo is depicted in Fig. 8 as an illustration. Here, x denotes the tissue depth from the skin surface, while y and z are along the surface.

The conditions at the boundaries of the cubic calculation domain in vivo are prescribed as follows:

$$-k \frac{\partial T}{\partial x} = h_f [T_f - T] \quad \text{at } x=0 \quad T = T_c \quad \text{at } x=L \quad (4)$$

$$-k \frac{\partial T}{\partial y} = 0 \quad \text{at } y=0 \quad -k \frac{\partial T}{\partial y} = 0 \quad \text{at } y=s_1 \quad (5)$$

$$-k \frac{\partial T}{\partial z} = 0 \quad \text{at } z=0 \quad -k \frac{\partial T}{\partial z} = 0 \quad \text{at } z=s_2 \quad (6)$$

where L is the distance between the skin surface and the body core; s_1 and s_2 are the widths of the tissue domain to be analyzed in the y and z directions, respectively; h_f is the convective heat transfer coefficient between the environment and the skin; and T_c , T_f are, respectively, the temperatures of the body core and the surrounding air.

The initial conditions of the cubic calculation domain in vivo are prescribed as follows:

$$T(x,y,z;0) = T_0(x) \quad (7)$$

here, $T_0(x)$ can be determined by solving the steady state Pennes equation [35]. The difference of boundary condition between in vitro and in vivo is that $-k(\partial T/\partial x)=0$ at $x=L$ in vitro, $T=T_c$ at $x=L$ in vivo, and the difference of initial condition between in vitro and in vivo is that $T(x,y,z;0)=T_f$ in vitro and $T(x,y,z;0)=T_0(x)$ in vivo.

The typical tissue properties are applied as given in Table 1 [36–39], and the probe and tumor domains used in calculations in vitro and in vivo are, respectively, defined in Table 2. The tissue dimension parameters are taken as $L=s_1=s_2=0.1$ m and the other demonstrative parameters are $h_f=10$ W/m² °C, $T_f=20$ °C, respectively.

In order to validate the theoretical model, comparison between the experimental results for in vitro pork and the corresponding numerical results is shown in Fig. 9, in which one 5 mm probe was used, with 10 min freezing and 5 min subsequent heating. In the calculation, the transient temperature response of probe tip was applied as the boundary condition at the surface of probe tip. Here, the transient temperature response of in vitro tissue at the position of about 2 mm from the probe tip was presented, and the initial temperature was about 24 °C. From the temperature curves either in the freezing or heating stage, it can be seen that the calculated values fit fairly well with the experimental data.

2.4 Theoretical Results for the Case of In Vitro Tissue. The probe and tumor domains for such case are shown in Table 2.

Table 1 Typical thermophysical properties of biological tissues [34–37]

	Unit	Value
Heat capacity of the frozen tissue	J/m ³ °C	1.8 × 10 ⁶
Heat capacity of the unfrozen tissue	J/m ³ °C	3.6 × 10 ⁶
Heat capacity of the blood	J/m ³ °C	3.6 × 10 ⁶
Thermal conductivity of the frozen tissue	W/m °C	2
Thermal conductivity of the unfrozen tissue	W/m °C	0.5
Latent heat	J/m ³	2.5 × 10 ⁸
Artery blood temperature	°C	37
Body core temperature	°C	37
Lower phase transition temperature	°C	-8
Upper phase transition temperature	°C	-1
Blood perfusion of normal tissue	ml/s ml	0.0005
Blood perfusion of tumor tissue	ml/s ml	0.002
Metabolic rate of normal tissue	W/m ³	4,200
Metabolic rate of tumor tissue	W/m ³	42,000

Here, cryoprobe perpendicular to the skin surface was pulled back 20 mm along the tract after the end of each freezing/heating cycle. The time for moving the probe was omitted. Experimental evidences have indicated that during the freezing/heating processes, the temperatures at the working tip of the probe can quickly reach a relatively stable value, which approximates to -196°C for freezing and 80°C for heating, respectively. Therefore, the temperature at probe tip is taken as $T_w = -196^\circ\text{C}$ during freezing, while $T_w = 80^\circ\text{C}$ during heating for the simulation.

Figure 10(a) gives the location and size of iceball at $t=600$ s when the first freezing cycle was finished. The interface between the iceball and the unfrozen tissue is determined by the isothermal surface of $T_{mi} = -1^\circ\text{C}$, and similarly hereinafter for the other calculation examples. The location and size of the iceball generated by a particular cryoprobe configuration are important in medical treatment, and its determination will allow the clinician to understand well the freezing necrosis extent as a result of applying a specific probe system. More importantly, such information is very beneficial for preselecting the correct probe parameters to realize a desirable lesion size. Figure 10(b) shows the location and size of iceball at $t=1260$ s when the second freezing cycle ends. At that time, the volume of the first iceball was decreased a little bit due to heating of surrounding environment while the volume of the second iceball is larger than the iceball formed at $t=600$ s because of the existence of first iceball. Figure 10(c) illustrates the final outcome with this new modality for in vitro samples. It is clear to

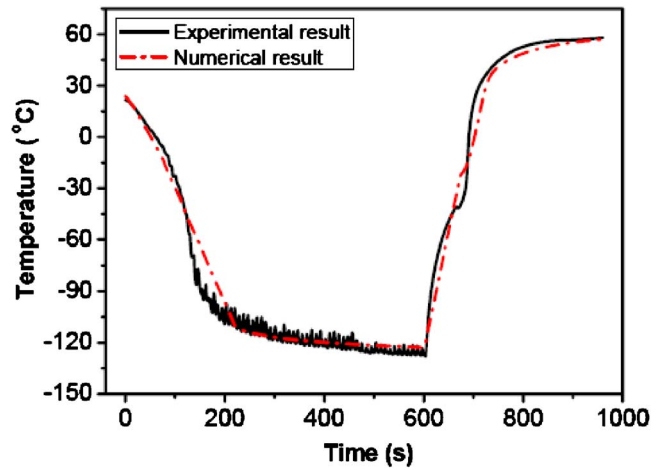


Fig. 9 Comparison between experimental and numerical results for in vitro pork

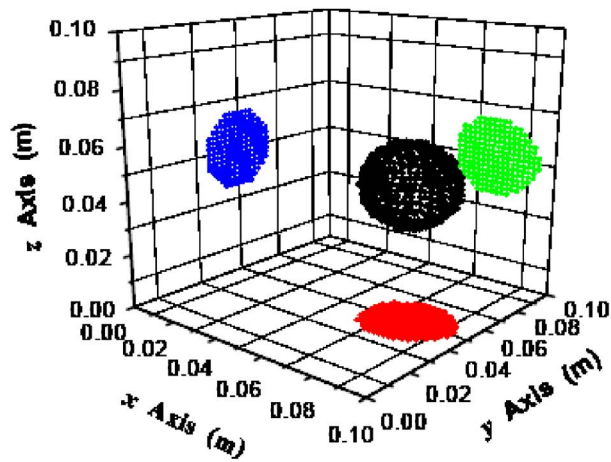
see that the iceballs were arranged in an order from big to small and an obvious icy gourd was formed. Such result is somewhat different from experimental outcome because the calculation boundary is close to the iceball, which implies that the heating effect of boundary on the freezing area cannot be ignored. In order to better illustrate the possible area of freezing injury using this new modality, the iceballs formed at different freezing cycles are overlapped together and shown in Fig. 10(d). It is clear to see that the calculations basically accord well with the experimental measurement.

2.5 Theoretical Results for the Case of In Vivo Tissue.

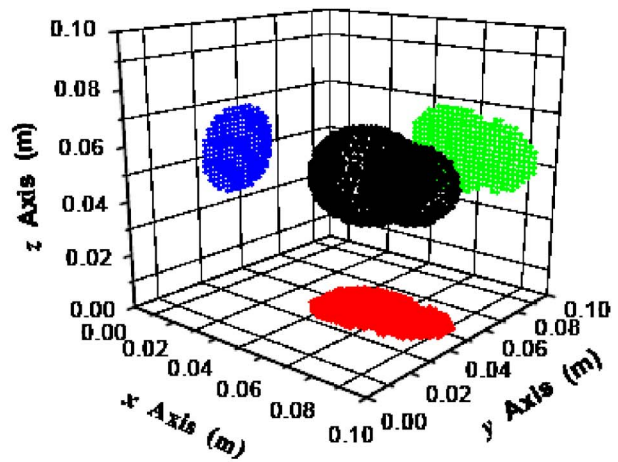
Here, cryoprobe was pulled back 14 mm along the tract after each freezing/heating cycle, and $T_w = -196^\circ\text{C}$ at freezing process, $T_w = 80^\circ\text{C}$ at heating process. Figure 11(a) presents the location and size of iceball at $t=600$ s when the first freezing cycle was finished. Due to the heating of metabolic heat generation and blood perfusion heat transfer in living tissues, the volume of iceball as indicated by Fig. 11(a) is smaller than that in Fig. 10(a) for the same freezing condition. Figures 11(b)–11(d) depict the iceballs formed at the second and third cycles and the overlapped iceballs of all cycles, respectively. Compared with the in vitro case, the outcome shows that by reasonably controlling the freezing/heating time, it is still possible to apply this new modality to generate a

Table 2 Probe and tumor domains used in calculations

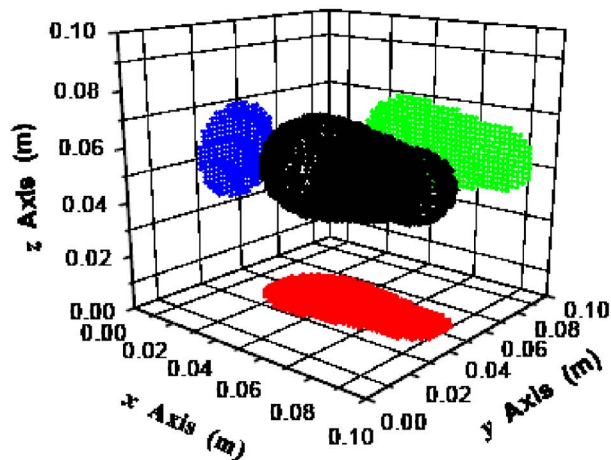
	Tumor domain	Probe domain	Procedure	
In vitro	None	0.070 m ≤ x ≤ 0.076 m	First freeze/heat cycle	Freezing 600 s Heating 60 s
		0.048 m ≤ y ≤ 0.052 m		
		0.048 m ≤ z ≤ 0.052 m		
		0.050 m ≤ x ≤ 0.056 m	Second freeze/heat cycle	Freezing 600 s Heating 60 s
		0.048 m ≤ y ≤ 0.052 m		
		0.048 m ≤ z ≤ 0.052 m		
		0.030 m ≤ x ≤ 0.036 m	Third freeze/heat cycle	Freezing 600 s Heating 60 s
		0.048 m ≤ y ≤ 0.052 m		
		0.048 m ≤ z ≤ 0.052 m		
In vivo	0.030 m ≤ x ≤ 0.072 m 0.045 m ≤ y ≤ 0.055 m 0.045 m ≤ z ≤ 0.055 m	0.070 m ≤ x ≤ 0.076 m	First freeze/heat cycle	Freezing 600 s Heating 60 s
		0.048 m ≤ y ≤ 0.052 m		
		0.048 m ≤ z ≤ 0.052 m		
		0.050 m ≤ x ≤ 0.056 m	Second freeze/heat cycle	Freezing 600 s Heating 60 s
		0.048 m ≤ y ≤ 0.052 m		
		0.048 m ≤ z ≤ 0.052 m		
		0.030 m ≤ x ≤ 0.036 m	Third freeze/heat cycle	Freezing 600 s Heating 60 s
		0.048 m ≤ y ≤ 0.052 m		
		0.048 m ≤ z ≤ 0.052 m		



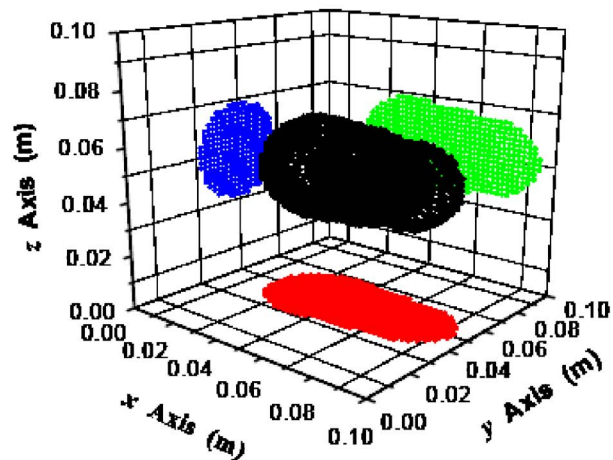
(a) Formation of first iceball at $t=600s$



(b) Formation of first and second iceballs at $t=1260s$



(c) Formation of first, second and third iceballs at $t=1920s$



(d) Superposed formation of first, second and third iceballs at $t=600s$, $1260s$ and $1920s$

Fig. 10 Subsequent formation of iceball during moving freezing in vitro

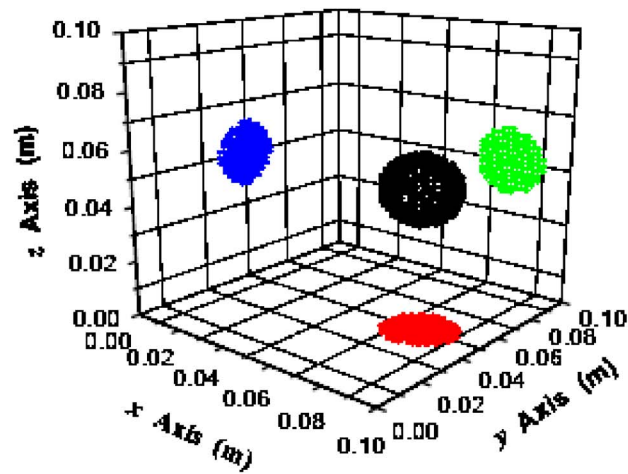
big enough iceball to acquire adequate surgical margin. To grasp a relatively complete picture of the new modality, the temperature profile along the maximum cross section of the iceball formation at $t=1920 s$ is also shown in Fig. 12. It can be seen that the isothermal lines do not take a regular elliptical shape but an elongated one, which is suitable in treating slender tumors. The guaranteed minimum killing radius (temperature zone below $-40^{\circ}C$) is about 0.5 mm while the maximum one is about 1 cm. In fact, the effective killing area could be larger due to the initial freezing iceball. Besides, this was formed only by one probe instead of multiple probes. That is to say, with this new modality, it is feasible to significantly minimize the numbers of cryoprobes while realizing a big icy entity to deal with slender tumors, which is superior to the conventional freezing methods.

3 Discussion

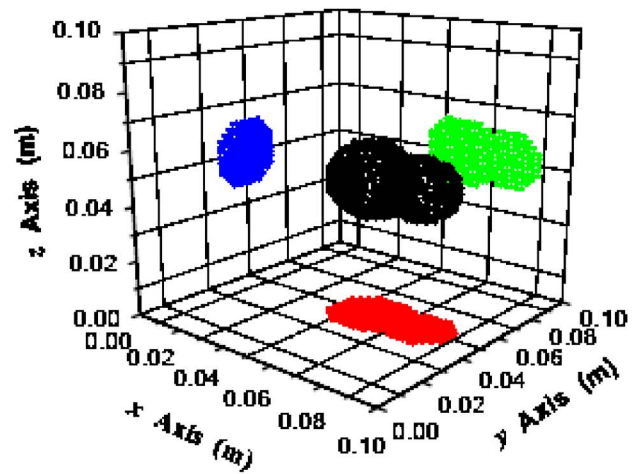
Cryosurgery is becoming an attractive treatment option for many tumors such as prostate, liver, kidney, and breast tumors primarily due to its minimally invasive nature. Moreover, many advanced image guidance systems such as ultrasound, computer tomography (CT), and magnetic resonance imaging (MRI) allow intraoperative monitoring of the iceball (and hence the area of treatment) surrounding the probes during cryosurgery, which is an advantage over many other minimally invasive treatments

[1–3,40]. However, there are still challenges to be addressed in improving the treatment efficacy. Some limitations as mentioned above make the existing cryosurgical instruments unable to ablate slender solid tumor effectively or produce a satisfactory effective coverage of iceball to treat complex anatomical structures via an easy and quick way. This may impede the broader use of conventional cryoprobe-based devices.

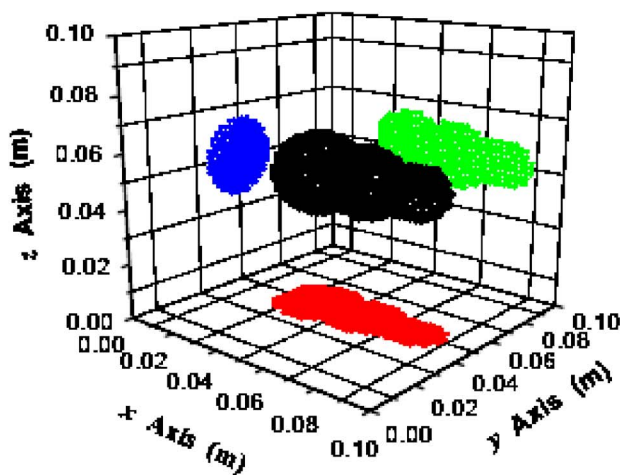
Through the way to increase the number of probes, the above problem can thus be solved to some extent. However, it has a potentially negative effect. For example, on the one hand, this would increase the difficulty and complexity of surgical operation; on the other hand, it could enlarge the additional mechanical incision lesions and increase the cost of medical care. One case reported based on prostate-specific antigen (PSA) result [41] is that a “cryoseed system” (Galil Medical Inc, Haifa, Israel) using more than 8 numbers of 17-gauge needle probes to create a 1 cm diameter iceball was found unable to totally ablate the prostate gland. The new conceptual modality as proposed in this paper could possibly resolve that difficulty without resulting in serious negative effect brought about by inserting too many probes. It should be pointed out that this new modality could still be extended to more forms, not only the cases reflected by the present experiments. With different combinations of the sizes and positions of probes, the freezing/heating duration time, and the mov-



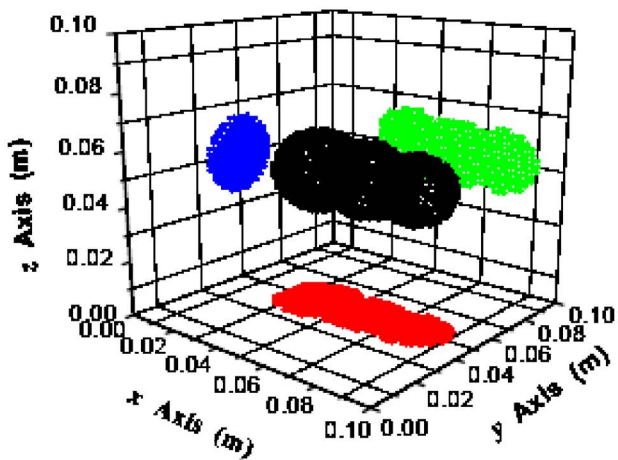
(a) First iceball formation when $t=600s$



(b) First and second iceballs formation when $t=1260s$



(c) Formation of first, second and third iceballs at $t=1920s$



(d) Superposed formation of first, second and third iceballs at $t=600s, 1260s$ and $1920s$

Fig. 11 Subsequent formation of iceball during moving freezing in vivo

ing distances of the probe, it is much more convenient and flexible to do with some special shapes of solid tumors. Moreover, for most of the conventional cryosurgery system, it is difficult to treat the tumor with a huge size [42]. However, according to the present experience, based on the combined freezing/heating system and by using the new modality, it is relatively easy to deal with the slender tumor whose size is over 5 cm because iceball could be conveniently accumulated to enwrap the tumor with this new modality. That is to say, pullback with one probe could meet the same demand via a much lower cost for curing large slender tumor as provided by conventional multiple probes.

Of course many factors should be considered before putting the present method into practice. In order to address the needs of a specific patient, the computer model must rely on the data reflecting the particular situation, namely, the layout of the tumor and the delicate organs or tissues that must be protected. In addition, it is much more important to appropriately operate with the new modality. This is because the freezing/heating time and moving distances along the tract would have important effects on the shape of a final iceball. A wrong operation may leave the target regions incompletely frozen while lead to freeze or thermal injury to the surrounding healthy tissue. In this article, we have developed a feasible way to simulate the new modality, which would

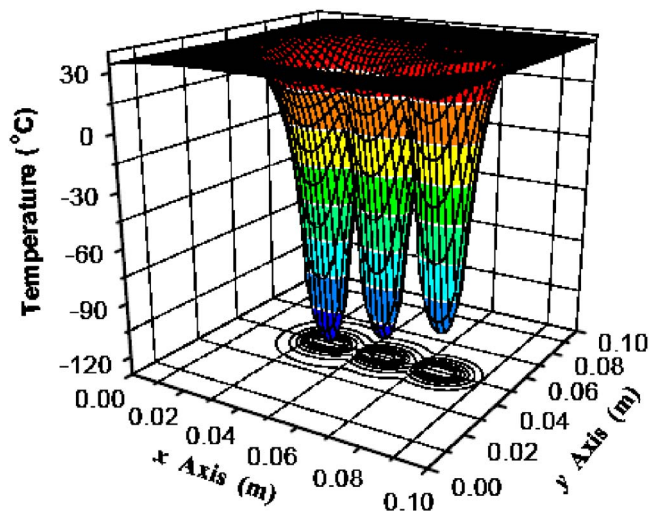


Fig. 12 Temperature profile in the maximum cross section of iceball formation at $t=1920s$ in vivo

provide both shape and temperature information of iceball. This will help clinicians to better understand the whole procedure of freezing/heating and design more reasonable cryosurgical plan. However, more thorough studies by incorporating more complex physiological or anatomical structures are still needed.

4 Conclusion

The minimally invasive approach will become more and more popular in cryosurgery, which offers considerable advantages to the patient. However, such technique could bring additional troubles. Up to date, the critical issues to efficiently freeze the large slender tumors while minimizing the mechanical lesions is still not well solved, especially with the increase of the number of cryoprobe. The present method was just proposed to partially overcome such difficulty. Both experimental tests and mathematical simulation demonstrated the feasibility of the new modality whose merits could be summarized as follows: (1) low trauma and risk of mechanical lesion due to avoidance of multiple probes' incision, (2) adapt to large tumor with slender shape, (3) multiple cycles of freezing/heating to increase killing efficacy through an appropriate combination among them, and (4) easy operation and practical utility for a pre-carefully-planned insertion path for the probe. In conclusion, the present modality is expected to provide the cryosurgeons more choices in performing a highly efficient minimally invasive cryosurgery.

Acknowledgment

This work was partially supported by the National Natural Science Foundation of China under Grant Nos. 50325622, 50576104, and 50436030. The authors wish to appreciate the very constructive help from the anonymous reviewers.

References

- [1] Ahmed, S., Lindsey, B., and Davies, J., 2005, "Emerging Minimally Invasive Techniques for Treating Localized Prostate Cancer," *Br. J. Urol.*, **96**, pp. 1230–1234.
- [2] Saliken, J. C., Donnelly, B. J., and Rewcastle, J. C., 2002, "The Evolution and State of Modern Technology for Prostate Cryosurgery," *Urology*, **60**, pp. 26–33.
- [3] Cooper, S. M., and Dawber, R. P., 2001, "The History of Cryosurgery," *J. R. Soc. Med.*, **94**, pp. 196–201.
- [4] Rubinsky, B., 2000, "Cryosurgery," *Annu. Rev. Biomed. Eng.*, **2**, pp. 157–187.
- [5] Onik, G., 2001, "Image-Guided Prostate Cryosurgery: State of the Art," *Cancer Control*, **8**, pp. 522–531.
- [6] Harada, J., and Mogami, T., 2004, "Minimally Invasive Therapy Under Image Guidance-Emphasizing MRI-Guided Cryotherapy," *Rinsho Byori*, **52**, pp. 145–151.
- [7] Edd, J. F., Horowitz, L., and Rubinsky, B., 2005, "Temperature Dependence of Tissue Impedivity in Electrical Impedance Tomography of Cryosurgery," *IEEE Trans. Biomed. Eng.*, **52**, pp. 695–701.
- [8] Choi, B., Milner, T. E., Kim, J., Goodman, J. N., Vargas, G., Aguilar, G., and Nelson, J. S., 2004, "Use of Optical Coherence Tomography to Monitor Biological Tissue Freezing During Cryosurgery," *J. Biomed. Opt.*, **9**, pp. 282–286.
- [9] www.pcds.org.uk/pdf/Cryosurgery%20for%20the%20GP%20and%20GP%20Specialist.pdf
- [10] Robinson, J. W., Saliken, J. C., Donnelly, B. J., Barnes, P., and Guyn, L., 1999, "Quality-of-Life Outcomes for Men Treated With Cryosurgery for Localized Prostate Carcinoma," *Cancer*, **86**, pp. 1793–1801.
- [11] <http://www.cryocare.com.cn>
- [12] Baust, J. G., and Gage, A. A., 2004, "Progress Toward Optimization of Cryosurgery," *Technol. Cancer Res. Treat.*, **3**, pp. 95–101.
- [13] Kyle, J. W., and Jaime, L., 2005, "Comparison of Cryoablation, Radiofrequency Ablation and High-Intensity Focused Ultrasound for Treating Small Renal Tumours," *Br. J. Urol.*, **96**, pp. 1224–1229.
- [14] http://www.nci.nih.gov/PDF/FactSheet/fs7_34.pdf
- [15] Gage, A. A., and Baust, J. G., 1998, "Mechanisms of Tissue Injury in Cryosurgery," *Cryobiology*, **37**, pp. 171–186.
- [16] Baust, J. G., and Gage, A. A., 2005, "The Molecular Basis of Cryosurgery," *Br. J. Urol.*, **95**, pp. 1187–1191.
- [17] Gage, A. A., and Baust, J. G., 2002, "Cryosurgery—A Review of Recent Advances and Current Issues," *Cryoletters*, **23**, pp. 69–78.
- [18] Zhang, Y. T., and Liu, J., 2002, "Numerical Study on Three-Region Thawing Problem During Cryosurgical Re-Warming," *Med. Eng. Phys.*, **24**, pp. 265–277.
- [19] Hoffmann, N. E., and Bischof, J. C., 2002, "The Cryobiology of Cryosurgical Injury," *Urology*, **60**(2), pp. 40–49.
- [20] Liu, J., Zhou, Y. X., Yu, T. H., Gui, L., Deng, Z. S., and Lv, Y. G., 2003, "New Cryoprobe System With Powerful Heating Features and Its Performance Tests on Biomaterials," *Proceedings of 2003 ASME IMECE: 2003 ASME International Mechanical Engineering Congress and RD&D Expo*.
- [21] Liu, J., Zhou, Y. X., Yu, T. H., Gui, L., Deng, Z. S., and Lv, Y. G., 2004, "Minimally Invasive Probe System Capable of Performing Both Cryosurgery and Hyperthermia Treatment on Target Tumor in Deep Tissues," *Minimally Invasive Ther. Allied Technol.*, **13**, pp. 47–57.
- [22] Peralta, A. H., Hollander, Y., Solazzo, S., Horkan, C., Liu, Z. J., and Goldberg, S. N., 2004, "Hybrid Radiofrequency and Cryoablation Device: Preliminary Results in an Animal Model," *J. Vasc. Interv. Radiol.*, **15**, pp. 1111–1120.
- [23] Zhang, Y. T., and Liu, J., 2002, "Study on Thermal Stress in Living Tissues During Cryosurgical Rewarming (in Chinese)," *Space Medicine & Medical Engineering*, **15**, pp. 291–295.
- [24] Han, K.-R., and Belldegrun, A. S., 2004, "Third-Generation Cryosurgery for Primary and Recurrent Prostate Cancer," *Br. J. Urol.*, **93**, pp. 14–18.
- [25] Zisman, A., Pantuck, A. J., Cohen, J. K., and Belldegrun, A. S., 2001, "Prostate Cryoablation Using Direct Transperineal Placement of Ultrathin Probes Through a 17-Gauge Brachytherapy Template—Technique and Preliminary Results," *Adult Urology*, **58**, pp. 988–993.
- [26] Hsiao, J. S., 1985, "An Efficient Algorithm for Finite-Difference Analyses of Heat Transfer With Melting and Solidification," *Numer. Heat Transfer*, **8**, pp. 653–666.
- [27] Pham, Q. T., 1986, "The Use of Lumped Capacitance in the Finite-Element Solution of Heat Conduction Problems With Phase Change," *Int. J. Heat Mass Transfer*, **29**, pp. 285–291.
- [28] Comini, G., Guidice, S. D., and Saro, O., 1990, "A Conservative Algorithm for Multidimensional Conduction Phase Change," *Int. J. Numer. Methods Eng.*, **30**, pp. 697–709.
- [29] Lee, R. T., and Chiou, W. Y., 1995, "Finite-Element Analysis of Phase Change Problems Using Multilevel Techniques," *Numer. Heat Transfer, Part B*, **27**, pp. 277–290.
- [30] Gong, Z. X., and Mujumdar, A. S., 1997, "Non-Convergence Versus Non-Conservation in Effective Heat Capacity Methods for Phase Change Problems," *Int. J. Numer. Methods Heat Fluid Flow*, **17**, pp. 565–579.
- [31] Amin, M. R., and Greif, D., 1999, "Conjugate Heat Transfer During Two-Phase Solidification Process in a Continuously Moving Metal Using Average Heat Capacity Method," *Int. J. Heat Mass Transfer*, **31**, pp. 2883–2895.
- [32] Amin, M. R., 2000, "Thermal Analysis During Continuous Casting Process Using Effective Heat Capacity Method," *J. Thermophys. Heat Transfer*, **14**, pp. 170–176.
- [33] Deng, Z. S., and Liu, J., 2004, "Modeling of Multidimensional Freezing Problem During Cryosurgery by the Dual Reciprocity Boundary Element Method," *Eng. Anal. Boundary Elem.*, **28**, pp. 97–108.
- [34] Deng, Z. S., and Liu, J., 2004, "Numerical Simulation on 3-D Freezing and Heating Problems for the Combined Cryosurgery and Hyperthermia Therapy," *Numer. Heat Transfer, Part A*, **46**, pp. 587–611.
- [35] Deng, Z. S., and Liu, J., 2002, "Analytical Study on Bioheat Transfer Problems With Spatial or Transient Heating on Skin Surface or Inside Biological Bodies," *ASME J. Biomech. Eng.*, **124**, pp. 638–649.
- [36] Rabin, Y., and Shitzer, A., 1998, "Numerical Solution of the Multidimensional Freezing Problem During Cryosurgery," *ASME J. Biomech. Eng.*, **120**, pp. 32–37.
- [37] Liu, J., and Wang, C. C., 1997, *Bioheat Transfer (in Chinese)*, Science Press, Beijing.
- [38] Chato, J. C., 1985, "Selected Thermophysical Properties of Biological Materials," in *Heat Transfer in Medicine and Biology*, Shitzer, A., and Eberhart, E. C. eds., Plenum, New York, pp. 413–418.
- [39] Deng, Z. S., and Liu, J., 2002, "Monte Carlo Method to Solve Multidimensional Bioheat Transfer Problem," *Numer. Heat Transfer, Part B*, **42**, pp. 543–567.
- [40] Singletary, S. E., 2002, "Minimally Invasive Ablation Techniques in Breast Cancer Treatment," *Ann. Surg. Oncol.*, **9**, pp. 319–320.
- [41] Rabin, Y., David, C. L., and Thomas, F. S., 2004, "Computerized Planning of Cryosurgery Using Cryoprobes and Cryoheaters," *Technol. Cancer Res. Treat.*, **3**, pp. 229–243.
- [42] <http://healthlink.mcw.edu/article/957905401.html>